analytical chemistry

Article

pubs.acs.org/ac

Generation−Collection Electrochemistry Inside a Rotating Droplet

Magdalena Kundys, Michal Nejbauer, Martin Jönsson-Niedziolka, and Wojciech Adamiak*

Institute of Physical Chemistry, Polish Academy of Sciences, Kasprzaka 44/52, 01-224 Warsaw, Poland

Supporting Information

ABSTRACT: In this work, we explore generation−collection electrochemistry in a rotating droplet hydrodynamic system, where a 70 μL droplet containing a redox active species (ferrocyanide) is sandwiched between an upper rotating rod and bottom nonmoving generator and collector planar electrodes. In such a system, we studied the effect of the counter electrode reaction on the recorded generator current, and the effect of the generator−collector distance (ranging from 3 to ca. 500 μm) on the collection efficiencies obtained at rotation rates ranging from 50 to 1100 rpm. We found that the counter electrode reaction competes with the collector reaction for the regeneration of the electroactive species; thus, collection efficiencies of 100% are probably impossible to obtain with this system geometry. We found that the collection efficiency increases with the droplet rotation rate and decreases with the generator−collector distance. The highest collection efficiency we obtained is 62% for the generator−collector distance of 3 μm, which is more than two times higher than that for typical bulk experiments with a commercial rotating ring disk electrode. We show that the increased collection efficiency can be successfully used in epinephrine detection for filtering out signals from ascorbic acid and uric acid interferents.

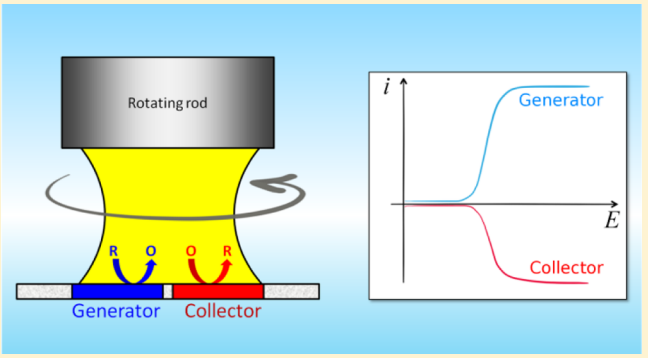

Accurate analysis of small liquid samples often requires their volume to be adjusted to the selected analytical method. This is usually performed by diluting the sample with either a dedicated solvent or a solvent mixture.[1−4] However, each sample dilution introduces an error to the analytical result, sometimes leading to considerable deviation between sample-to-sample probing.[5,6] For example, Franklin et al. have shown that different dilution procedures can significantly affect genetics, physiology, and morphology of cell cultures grown from the same sewage environment,[7] whereas Higgins et al. discussed the effect of serial dilution errors on calibration curves in immunoassay techniques.[8] To eliminate dilution errors, efforts are made to perform analysis directly in small samples, some of them taking advantage of droplet confinement of the sample. These require sometimes highly sophisticated equipment and skillful personnel for data interpretation.[9−17]

For redox active samples, simple instrumentation is offered by electrochemical methods. Typical electrochemical measurements are made with widely available PC-controlled potentiostats, whose size and weight have been continuously reduced over recent decades, so now the equipment is easily portable with high sensitivity maintained. Also, typical electrochemical measurements by cyclic voltammetry at moderate scan rates take a few minutes with the only requirement the sample must meet being sufficiently high ionic conductivity to support the flow of the electric current (though, with the use of microelectrodes, even this limitation has been overcome).[18−21]

With respect to electroanalysis, a small sample volume provides favorable conditions for highly sensitive methods based on bulk electrolysis processes, where all target molecules undergo electrochemical reactions, either to contribute to the analytical signal or to selectively remove the interferent molecules from the solution (electroseparation). In the first case, electrogravimetric and coulometric techniques have been developed[22−36] and used for both detection purposes (such as for detection of steroids[22] or neurotransmitters[23]) as well as for characterizing materials (such as conducting polymers,[24] nanocomposites,[25] solid propellants,[26] or photocatalysts[27,28]). Examples of electroseparation have involved recovery of chromic acid and metal ions,[29] separation of Co and Ni from wastewater,[30] Th from ThO_2, and La_2O_3[31] or Ag from Pd.[32] Apart from the purely analytical benefits that the small volume brings to electrochemistry, it also allows one to increase the yield of electro-organic reactions,[33−36] because all reagents are likely to reach the electrode surface within a short period of time without the need for bulk solution mixing.

One of the recently reported methods that combines small-volume environment together with electrochemistry is the so-called rotating droplet (RD) method, where a microliter volume solution is sandwiched between an upper rotating rod (standard rotating disk electrode, RDE, or rotating ring disk electrode, RRDE, tips can be used for that purpose) and a bottom nonmoving electrode surface[37,38] (a pioneering work on a similar technique where the droplet was rotated by mild

Received: April 26, 2017
Accepted: July 5, 2017
Published: July 5, 2017

DOI: 10.1021/acs.analchem.7b01533
Anal. Chem. 2017, 89, 8057−8063

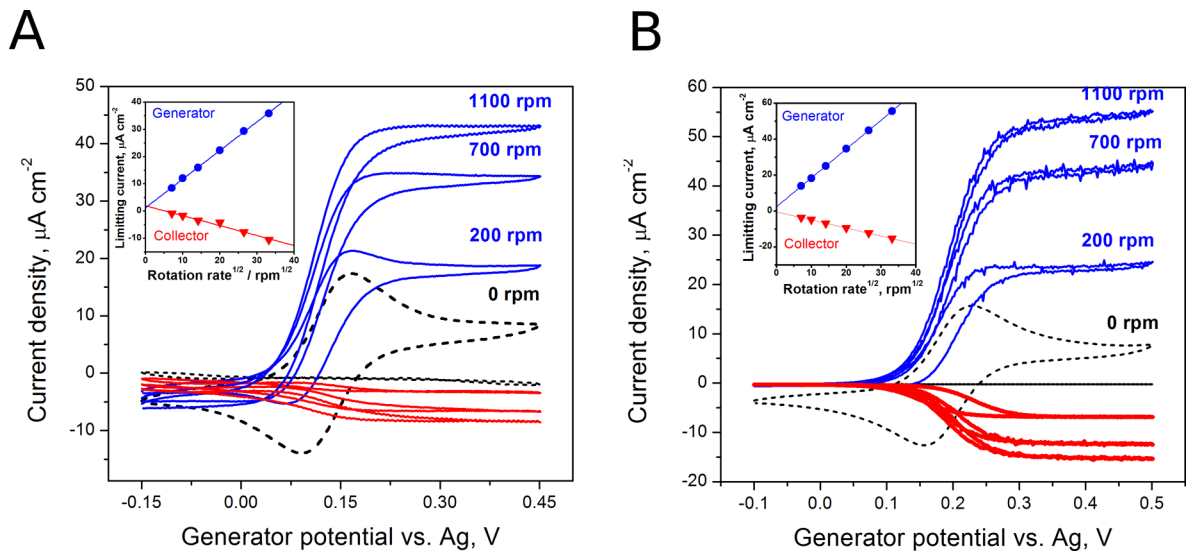

Figure 1. CV–CA signals for rotating droplet (RD; A) and rotating ring disk electrode (RRDE; B) at different rotation rates. The insets show Levich plots for the generator and collector limiting currents as a function of the square root of the rotation rate. The scan rate of the CV was 25 mV/s. The solution was 1 mM $K_4[Fe(CN)_6]$ + 0.1 M KNO_3. The generator–collector distance was 18 μm in RD and 1 mm in the commercial RRDE tip. The collector CA potentials were −0.15 and −0.1 V for RD and RRDE methods, respectively.

gas flow was reported by Cserey and Gratzl).[39] With respect to the hydrodynamic environment generated by the rotating tip, the method seems similar to the standard rotating disk electrode (RDE), but it works with only a few tens of microliters of sample solution (not several milliliters, as in the case of RDE). It also allows using electrode materials that are different from those of which commercially available RDE tips are made. In 2013, Chalier et al. used the RD technique to study reaction kinetics for real-time monitoring of the biological reactions,[37] whereas in 2016 our group showed that it is also possible to use RD for gaseous sample probing.[38] The main advantage of the RD technique over other static electroanalytical methods is the higher current response due to the convective mass transport forced by the spinning droplet.

In this work, we further explore the RD technique and discuss generation–collection electrochemistry in this new hydrodynamic volume-limited environment. Numerous generation–collection systems—where the signal recorded on one electrode (generator) is amplified due to the reversed reaction on a second electrode (collector)—have been studied, ranging from static interdigitated electrodes[40−45] or nanogap electrodes[46−50] through microfluidic channels[51−55] and rotating ring disk electrodes,[56−60] but none of them has dealt with both small droplet confinement and droplet rotation. Here, we discuss the effect of the generator–collector distance and counter electrode reactions on the total current recorded on the generator. In contrast to the typically designed electrochemical cells, where the distance between the counter electrode and working electrode is large and the counter electrode reactions are neglected, in the RD method, the counter electrode is close to both generator and collector electrodes, and thus it acts as a second collector electrode. To probe this effect, we performed experiments under static conditions with microtrench electrodes that allow us to position the counter electrode in micrometer distance from the generator electrode. We also discuss practical aspects of the electrode preparation and compare the results obtained on the electrodes prepared by either simple mechanical scratching of the ITO surface (suitable for preparing a generator–collector gap size of hundreds of micrometers) or by laser ablation (suitable for preparing a gap size of a few micrometers). This is another advantage of RD over RRDE; i.e., one can prepare gaps of different sizes which is impossible with commercially available RRDE tips with predefined ring–disk distances. The most important result, from an analytical application point of view, is that in our system we obtained a collection efficiency of >60% which is more than two times higher than the ca. 25% achieved in a large-volume RRDE experiment.

MATERIALS AND METHODS

Chemicals and Materials. $K_4Fe(CN)_6$, KNO_3, $AgNO_3$, Na_2HPO_4, and NaOH were purchased from POCh, Poland. *N*-((Trimethoxysilyl)propyl)-*N*,*N*,*N*-trimethylammonium (TMA) chloride in methanol (50%) was purchased from ABCR, Germany. Uric acid (UA), epinephrine (EP), tetramethoxysilane (TMOS), and ammonium 2,2′-azinobis(3-ethylbenzothiazolinesulfonate) ($(NH_4)_2(ABTS^{2-})$) were purchased from Sigma-Aldrich. Ascorbic acid (AA) was from Riedel-de Haën. Emperor 2000 carbon nanoparticles with phenylsulfonate functionalities (CNPs) were obtained from Cabot Corp. All reagents were used as received. Indium tin oxide (ITO) coated glass plates (resistivity, 8–12 Ω sq^{-1}) were purchased from Delta Technologies, Ltd., USA.

Fabrication of the Generator and Collector Electrodes on ITO. First, the ITO slides (25 mm × 50 mm × 1.1 mm) were cleaned with acetone, isopropanol, ethanol, and deionized water. To remove any organic residues, they were next heated for 10 min in a tube furnace at 500 °C. To obtain two working electrodes placed closely one to each other, either the ITO plates were scratched mechanically with a diamond knife or they were cut using laser ablation. A home-built laser generated a train of 200 fs pulses at a central wavelength of 1030 nm, average power of 100 mW, and 600 kHz repetition rate. The beam was focused by an aspheric lens of 20 mm focal length to a spot of around 4 μm (Gaussian beam waist size). Samples were mounted on a motorized translation stage connected with a manual tilt platform to ensure that the stage axis was perpendicular to the beam direction. A pattern of straight lines

DOI: 10.1021/acs.analchem.7b01533
Anal. Chem. 2017, 89, 8057–8063

was created across the sample at a speed of 100 mm/s of the translation stage and the laser beam turned on. By varying the position of the sample with respect to the beam waist and adapting the laser pulse energy, we were able to create lines with different widths: 3, 18, 33, 150, 325, 415, and 487 μm (see Supporting Information Figure S1). The gap widths were measured under optical microscope. Modification of ITO with CNP-TMA matrix was done according to the procedure described by Rozniecka et al.[61] As a result of the modification, both the ITO generator and collector were covered by a heterogeneous layer of carbon-like material (see Figure S2) on which reversible oxidation of epinephrine was possible.

Fabrication of the Microtrench Electrodes. The trench electrodes were made from ITO coated glass (10 × 50 mm^2) that was cut at a 45° angle and assembled in a V-shape with the ITO surfaces facing each other. Scotch Magic Tape was used as a spacer with a rectangular active electrode area cut out using scissors. The electrodes were fixed together using a cyanoacrylate glue, and the edges were secured from leaking using nail varnish. The distance between the electrode surfaces was measured under an optical microscope (Nikon Eclipse LV150) to 55 ± 2 μm.

Electrochemical Measurements. Electrochemical measurements were performed using an Autolab PGSTAT30 (Metrohm Autolab) electrochemical system. The RDE system and Pt−Pt RRDE tips were purchased from ALS. The area of the ITO was masked by a hydrophobic tape. The generator and collector electrodes were either bare ITO or ITO modified with CNP-TMA matrix. Platinum RRDE was used as the counter (ring) electrode. The reference electrode was made by depositing Ag on the Pt disk of the RRDE via cyclic voltammetry scanning in a 20 mM solution of $AgNO_3$ in 10 mM NaOH, 30 scans from −0.1 to 0.1 V. The ITO plate with a masked area was placed at the bottom while the RRDE tip was placed at the top. Using a micropipette, a 70 μL droplet containing the electroactive analyte was gently injected between the electrodes with surface tension keeping it in a droplet shape. All experiments were conducted at 20 ± 2 °C.

RESULTS AND DISCUSSION

Voltammetric Characterization. Figure 1A shows the results of typical generation−collection measurements with a droplet containing $Fe(CN)_6^{4-}$ as a model redox compound. In the experiment, we performed cyclic voltammetry (CV) on the generator and simultaneously chronoamperommetry (CA) on the collector. The electrode reactions at both electrodes were as follows:

generator:

$$Fe(CN)_6^{4-} - e^- \rightarrow Fe(CN)_6^{3-}$$

collector:

$$Fe(CN)_6^{3-} + e^- \rightarrow Fe(CN)_6^{4-}$$

When the droplet was not rotating (dashed curve in Figure. 1A), the generator voltammogram exhibited well-defined anodic and cathodic peaks with anodic-to-cathodic peak current ratio of ca. 1 and peak separation close to 60 mV. These features confirm electrochemical reversibility of the $Fe(CN)_6^{4/3-}$ redox couple reported earlier.[62,63]

As the rotation rate increased, the peaks changed into a wave-like response due to the increased convection forced by the rotating tip. At rotation rates higher than 200 rpm, purely convective mass transport with no diffusion peaks was observed for the generator. Also, as the rotation rate increases, the collector limiting current increased due to more effective mass transport from the generator. Both the generator and collector limiting currents depend linearly on the square root of the rotation rate (inset in Figure. 1A) as expected in agreement with the classic Levich equation:[64]

$$j_{lim} = \alpha n F D^{2/3} \omega^{1/2} \nu^{-1/6} C$$

where j_{lim} is the limiting current density (A/cm^2), α is a parameter characteristic for a given hydrodynamic method (e.g., 0.620 for RDE), n is the number of electrons transferred in the reaction, F is the Faraday constant (C/mol), A is the electrode area (cm^2), D is the diffusion coefficient of the electroactive species (cm^2/s), ω is the angular rotation rate (rad/s), ν is the kinematic viscosity of the solution (cm^2/s), and C is the concentration of the electroactive species (mol/cm^3).

Linear dependence of i_{lim} vs $\omega^{1/2}$ was also observed for the standard RRDE experiments with a few hundred times larger solution volume (Figure 1B), which suggests that hydrodynamic conditions for generation−collection electrochemistry in the RD method are similar to those in the bulk RRDE experiment. However, the slopes of Levich plots for RD (0.84 and 0.29 μA cm^{-2} rpm$^{-1/2}$ for the generator and the collector, respectively) are ca. 2 times lower than the slopes for RRDE (1.60 and 0.44 μA cm^{-2} rpm$^{-1/2}$ for the generator and the collector, respectively) , which agrees well with earlier reports[37,38] and reflects less effective mass transport to the electrode surface in RD than in RRDE.

Current amplification. In principle, generation−collection electrochemistry affords amplification of the generator current due to the redox cycling between the generator and collector electrodes.[44,45,49] It means that the generator current strongly depends on the collector reaction, and because of that, one cannot use it for determination of the standard rate constants as it is commonly done for classic RDE by plotting a so-called Koutecky−Levich plot. However, in our system for all the generator−collector distances (3, 18, 33, 150, 325, 415, and 487 μm) and for rotation rates ranging from 50 to 1100 rpm, the difference in the generator currents when the collector was ON and OFF was less than a few percent, meaning that the collector reaction does not affect the generator current. Lack of current amplification on the generator should then allow one to apply the Koutecky−Levich method to determine the standard rate constant of the electroactive species.[65−67]

Figure 2 shows the Koutecky−Levich plot for the generation reaction of the $Fe(CN)_6^{4-/3-}$ couple. Indeed, the dependence of i^{-1} vs $\omega^{-1/2}$ is linear with the intercept given by[64]

$$\text{intercept} = \frac{1}{FAkC}$$

where k is the standard rate constant. By taking the intercept = 51576 A^{-1} (rad s^{-1})$^{1/2}$, F = 96485 C mol^{-1}, A = 0.08 cm^2, and C = 10^{-6} mol cm^{-3}, we calculate k for $Fe(CN)_6^{4-/3-}$ to be 0.003 cm/s. Although, there are no reports on the standard rate constant for $Fe(CN)_6^{4-/3-}$ at ITO electrodes, the value of 0.003 cm/s is still within the range of rate constants reported for other materials,[68] which shows the usefulness of the generation−collection RD method for kinetic studies.

Lack of current amplification in a wide range of generator−collector distances and rotation rates, together with high collection efficiencies discussed in the next section, suggests

DOI: 10.1021/acs.analchem.7b01533
Anal. Chem. 2017, 89, 8057−8063

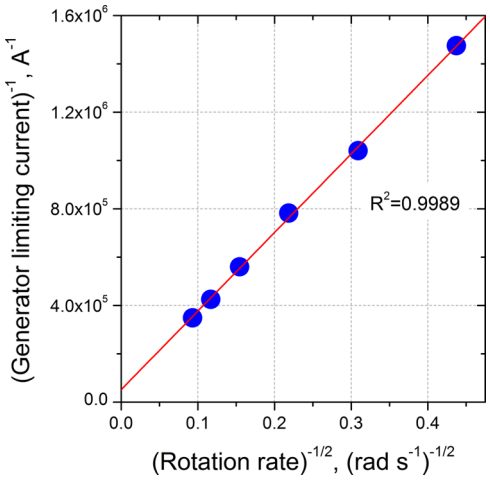

Figure 2. Koutecky–Levich plot for the generator limiting current recorded in the CV-CA measurement for generator–collector distance of 18 μm.

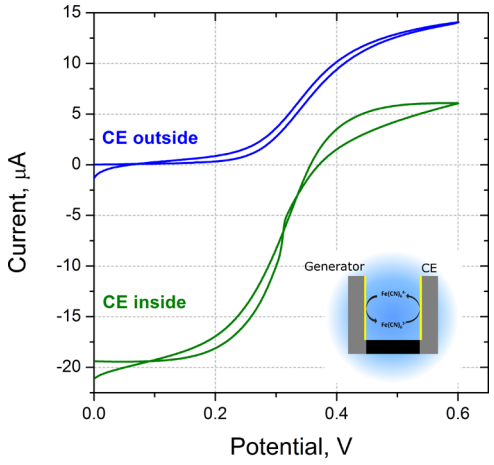

Figure 3. Cyclic voltammograms of 1 mM $K_4[Fe(CN)_6]$ recorded on the generator trench electrode when the counter electrode (CE) was either inside or outside the trench.

that the mass transport profile inside the rotating droplet allows the products formed on the generator to reach the collector electrode, but it prevents the collector products from reaching back to the generator. Such a mass transport profile does not give effective redox cycling and is similar to the one for RRDE and the one suggested by Chalier et al. for RD.[37] To determine the actual mass transport profile inside the rotating droplet, we are currently doing measurements with particle image velocimetry technique supported by COMSOL simulations of generation–collection electrochemical processes.

Counter Electrode Effect on the Generation–Collection Electrochemistry. A distinctive feature of a small-volume electrochemical system is the close vicinity of the counter electrode to the working electrode. Depending on the distance between the counter and working electrodes, the electroactive species formed on the working electrode can reach the counter electrode where they can be electrochemically regenerated. In this scenario, the counter electrode acts as a second collector electrode, and the reaction on the counter electrode should decrease the collection efficiency measured as a ratio between the "real" collector current and the generator current. To verify this theory and determine the effect of the counter electrode position on the generator response, we performed experiments under static conditions with microtrench electrodes where we changed the position of the counter electrode with respect to the generator electrode. Typical microtrench electrode consists of two oppositely faced ITO electrodes with an electrode-to-electrode distance of 55 μm.

When one of the ITO electrodes inside the trench was used as a counter electrode, meaning that the distance between the counter electrode and the generator electrode was ca. 50 μm, the generator voltammogram shows a distinct cathodic part (Figure 3, green curve), suggesting the presence of $Fe(CN)_6^{3-}$ in the trench. This $Fe(CN)_6^{3-}$ is likely to be formed on the counter electrode which appears to be polarized to sufficiently positive potential for $Fe(CN)_6^{4-}$ to be oxidized to $Fe(CN)_6^{3-}$. This preoxidation of $Fe(CN)_6^{4-}$ to $Fe(CN)_6^{3-}$ on the counter electrode, followed by reduction of $Fe(CN)_6^{3-}$ on the generator, gives rise to the observed cathodic current at low generator potentials. We see the same behavior in redox experiments using the RD system.[38] On the other hand, when the counter electrode is outside the trench, i.e., the distance between the generator and collector is a few centimeters, almost no cathodic current at low generator potentials is observed.

To visualize if the reagents formed on the bottom generator electrode can indeed reach the upper counter electrode in our generation–collection RD system,, we performed experiments where we oxidized $ABTS^{2-}$ to ABTS (which gives green color to the solution) on the generator and looked to see if the neutral ABTS can reach the upper counter electrode when the droplet was rotating (Figure 4). At 200 rpm, we see a green flux

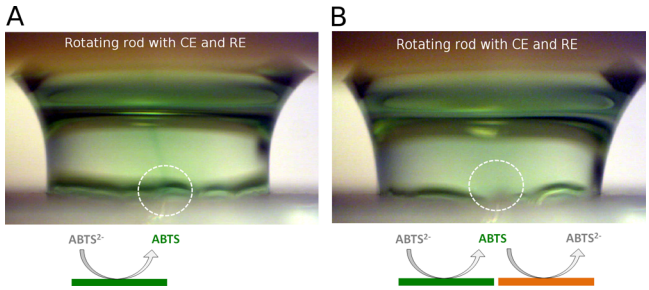

Figure 4. Photographs of $ABTS^{2-}$ oxidation to ABTS inside the rotating droplet when the collector is OFF (A) and when the collector is ON (B). The rotation rate was 200 rpm. The circles indicate the interelectrode gap between the generator and the collector.

of neutral ABTS in the vicinity of the upper counter electrode, which should allow the counter electrode to work as a second collector in the RD method, probably leading to smaller collection efficiencies. When the collector is OFF (Figure 4A), a homogeneous green glow can be seen close to the whole bottom surface of the droplet, including the interelectrode gap. When it is ON (Figure 4B), no green glow in the vicinity of the interelectrode gap can be seen, indicating consumption of the ABTS and regeneration of colorless $ABTS^{2-}$. The latter observation suggests that even when the counter electrode works as a collector electrode, we can still expect to record bottom collector response (which agrees with Figure 1 showing the collector CA signal), although collection efficiencies close to 100% are probably difficult to obtain (see next section).

Figure 4 shows one more important feature; i.e., when the droplet is rotating, the green color is more intense close to the bottom electrode surface than it is in the middle part of the

DOI: 10.1021/acs.analchem.7b01533
Anal. Chem. 2017, 89, 8057–8063

droplet. This observation indicates that (i) droplet rotation homogenizes its content in the center, but (ii) the concentration of electroactive ABTS species is higher close to the electrode surface. The latter feature can be attributed to less effective mass transport due to lower velocities close to the surface, suggested earlier by Noel et al.[37] and our group[38] and reflected in this work by lower slopes of the Levich plots in Figure 1A.

Collection Efficiency. To fully characterize generation−collection electrochemistry in a rotating droplet environment, we studied the effect of the generator−collector distance and the droplet rotation rate on the collection efficiency. Although, in the previous section, we have highlighted that the counter electrode acts as a competitive collector electrode, we still define the collection efficiency in a traditional way, i.e., a ratio between the current recorded on the bottom collector electrode and the current recorded on the bottom generator electrode. Such a definition allows us to compare our collection efficiencies to those reported in the literature for other hydrodynamic systems.

As shown in Figure 5, for all the gap sizes tested, the collection efficiency increases with the rotation rate, in contrast

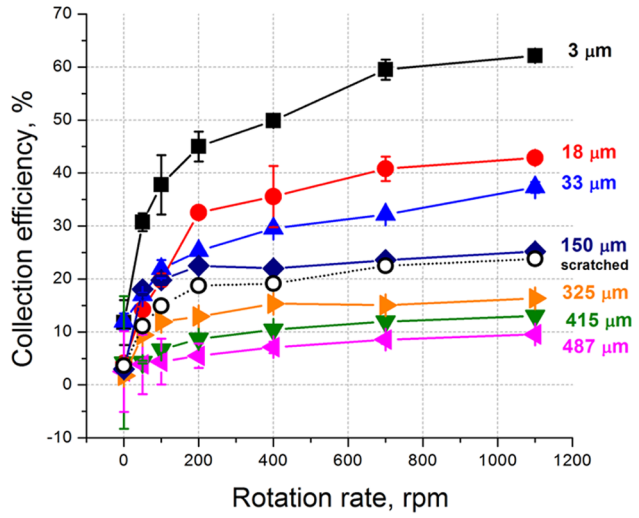

Figure 5. Collection efficiencies obtained for different generator−collector distances, plotted as a function of the rotation rate.

to the behavior in a RRDE system, where the collection efficiency is independent of rotation rate.[64]

A possible explanation for this is that the flow over the electrodes at the bottom of the droplet behaves oppositely to the flow over an RDE. That is, in the RD the flow comes down along the water−air interface and up, toward the rotating rod, in the center of the droplet (see Figure 4A). That means that if the rotation rate is high, so that the radial component of the flow is greater, more product is transported over to the collector instead of being lifted off toward the CE. This effect will be further investigated using particle image velocimetry method (PIV) and COMSOL simulations.

The highest collection efficiency that we have obtained is nearly 65% for the 3 μm generator−collector distance and rotation rate of 1100 rpm. This value is more than two times higher than the 27% we obtained with our commercially available RRDE tips.[69]

Since the collection efficiency is mainly determined by the generator−collector distance, we also tested simple mechanical scratching of the ITO slide as an alternative method to laser ablation for preparing the interelectrode gap. The smallest gap size we were able to prepare was ca. 150 μm, and the highest collection efficiency measured in RD was 25%. The latter value, together with the dependence of the collection efficiency on the rotation rate (Figure 5, empty circles), agrees well with the collection efficiency measured for 150 μm gap made by laser ablation (Figure 5, diamonds). Clearly, when high collection efficiencies are desired, more sophisticated methods than scratching for gap preparations must be involved, yet for qualitative generation−collection electrochemistry purposes, a preparation method as simple as mechanical scratching of the ITO surface can be used.

Detection of Epinephrine: Filtering out the Interferents. To demonstrate advantages of the generation−collection electrochemistry over typical voltammetry with single working electrode, we modified the generator and collector electrodes with a silicate hybrid matrix and performed detection of epinephrine in the solution containing common interferents, i.e., ascorbic acid and uric acid. Both interferents are present in real biological samples and undergo irreversible oxidation on appropriate carbon material.

Using a single working electrode, it is impossible to detect EP in the presence of AA and UA, because oxidation of EP occurs at higher potentials than oxidation of AA (which means that it is always preceded by the oxidation of AA) and redox potential of UA is close to that of EP, so the current signals from all three species overlap (see the inset in Figure 6A).

However, taking advantage of reversible electron transfer reactions of EP, and using generation−collection electrochemistry, it should be possible to simultaneously oxidize EP, AA, and UA at the generator electrode and at the same time reduce only EP^+ on the collector (inset in Figure 6B). In this way, the collector reaction will give the signal from the desired analyte, whereas the generator reaction will filter out the interferents.

Indeed, when the generator is polarized to 0.6 V and the collector is polarized to −0.2 V, the anodic and cathodic current transients are recorded on the generator and collector, respectively (Figure 6B). For a given rotation rate, the collector limiting current is proportional to the EP concentration (Figure 6C), indicating that it originates from electrochemical reduction of the EP^+ species formed on the generator. For all rotation rates tested, this dependence is close to linearity, with a sensitivity (slope) being the highest for 1100 rpm due to a more efficient mass transport rate between the generator and the collector. More efficient mass transport at higher rotation rates has been reflected earlier in the highest collection efficiency for this rotation rate (Figure 5). Certainly, the EP detection methodology needs further improvement with respect to the generator−collector distance, electrode modification procedure, droplet volume, or droplet height, yet it proves applicability of the generation−collection RD in electroanalysis. Development of the fully optimized RD-based electrochemical sensor for EP is, however, beyond the scope of this work.

CONCLUSIONS

In this work, we have demonstrated generation−collection electrochemistry inside a single rotating droplet. We have found that the collector current follows Levich-type behavior within

DOI: 10.1021/acs.analchem.7b01533
Anal. Chem. 2017, 89, 8057−8063

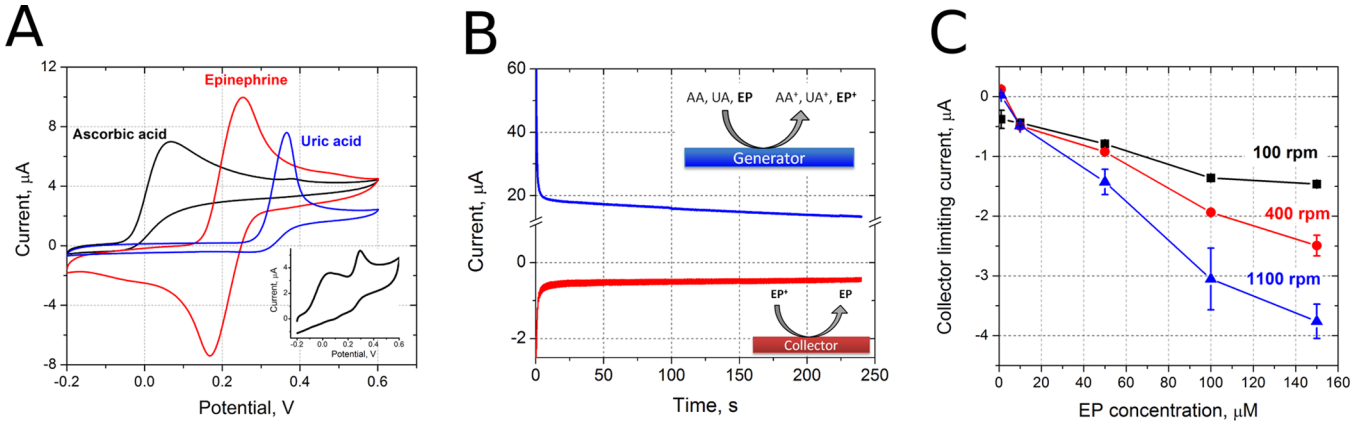

Figure 6. (A) Cyclic voltammograms of 1 mM ascorbic acid (AA), 2 mM epinephrine (EP), and 1 mM uric acid (UA) recorded in RD at 0 rpm on CNP-TMA-modified generator electrode. Inset: Cyclic voltammogram recorded in the mixture of 1 mM AA, 2 mM EP, and 1 mM UA at 0 rpm. (B) Typical chronoamperograms (CA–CA signals) recorded on the generator and collector at 1100 rpm for 10 μM EP, 0.5 mM AA, and 0.5 mM UA. The generator and collector potentials were 0.6 and −0.2 V, respectively. The inset shows the mechanism of filtering out the interferents. The generator–collector distance was 6 μm. (C) Dependence of the collector limiting current on the EP concentration for different rotation rates.

the studied rotation range. The collector electrode competes with the counter electrode for regeneration of the electroactive species formed on the generator electrode; thus, collection efficiencies close to 100% seem to be difficult to obtain. The highest collection efficiency we have obtained is 62% for generator–collector distance of 3 μm which is still more than two times higher than for RRDE experiment. We have shown that the high collection efficiency can be used for filtering out the interferents signal from the analyte signal in epinephrine detection. Although the collection efficiencies in the rotating droplet method are rather high, the system does not give current amplification from the redox cycling. The lack of current amplification suggests that the rotating droplet does not provide hydrodynamic conditions favorable for effective redox cycling, and that is why it is crucial to understand the mass transport inside the droplet. Once we know exactly how the molecules move upon droplet spinning, we will be able to tune the system so it will give not only high collection efficiency but also the significant current amplification, so much desired in a small-volume sample analysis.

■ ASSOCIATED CONTENT

Supporting Information

The Supporting Information is available free of charge on the ACS Publications website at DOI: 10.1021/acs.analchem.7b01533.

Scanning electron microscopy images of interelectrode gaps fabricated by laser ablation and of CNP-TMA-modified ITO electrode (PDF)

■ AUTHOR INFORMATION

Corresponding Author

*E-mail: wadamiak@ichf.edu.pl. Tel.: +48 223433306.

ORCID

Martin Jönsson-Niedziolka: 0000-0001-5642-5946

Wojciech Adamiak: 0000-0002-3875-2035

Author Contributions

M.K. performed all electrochemical experiments with RD technique, M.N. performed laser ablation experiments, M.J.-N. performed electrochemical experiments with trench electrodes and planned the experiment with EP, W.A. planned RD experiments and wrote the manuscript. All authors have given approval to the final version of the manuscript.

Notes

The authors declare no competing financial interest.

■ ACKNOWLEDGMENTS

Financial support from Polish National Science Center through Grant NCN 2014/15/D/ST4/03003 is acknowledged and greatly appreciated.

■ REFERENCES

(1) Ternes, T. A. *TrAC, Trends Anal. Chem.* **2001**, *20*, 419–434.

(2) Lankford, S. M.; Bai, S. *J. Chromatogr., Biomed. Appl.* **1995**, *663*, 91–101.

(3) Bodour, A. A.; Miller-Maier, M. M. *J. Microbiol. Methods* **1998**, *32*, 273–280.

(4) Nielsen, U. B.; Cardone, M. H.; Sinskey, A. J.; MacBeath, G.; Sorger, P. K. *Proc. Natl. Acad. Sci. U. S. A.* **2003**, *100*, 9330–9335.

(5) Gaines Das, R. E. *Clin. Chem.* **1980**, *26*, 1726–1729.

(6) Nicodemo, A. C.; Araujo, M. R. E.; Ruiz, A. S.; Gales, A. C. *J. Antimicrob. Chemother.* **2004**, *53*, 604–608.

(7) Franklin, R. B.; Garland, J. L.; Bolster, C. H.; Mills, A. L. *Appl. Environ. Microbiol.* **2001**, *67*, 702–712.

(8) Higgins, K. M.; Davidian, M.; Chew, G.; Burge, H. *Biometrics* **1998**, *54*, 19–32.

(9) Lin, Y.; Schiavo, S.; Orjala, J.; Vouros, P.; Kautz, R. *Anal. Chem.* **2008**, *80*, 8045–8054.

(10) Hatakeyama, T.; Chen, D. L.; Ismagilov, R. F. *J. Am. Chem. Soc.* **2006**, *128*, 2518–2519.

(11) Moon, H.; Wheeler, A. R.; Garrell, R. L.; Loo, J. A.; Kim, C.-J. *Lab Chip* **2006**, *6*, 1213–1219.

(12) Wheeler, A. R.; Moon, H.; Bird, C. A.; Ogorzalek Loo, R. R.; Kim, C.-J.; Loo, J. A.; Garrell, R. L. *Anal. Chem.* **2005**, *77*, 534–540.

(13) Fornell, A.; Nilsson, J.; Jonsson, L.; Periyannan Rajeswari, P. K.; Joensson, H. N.; Tenje, M. *Anal. Chem.* **2015**, *87*, 10521–10526.

(14) Nilsson, J.; Evander, M.; Hammarstrom, B.; Laurell, T. *Anal. Chim. Acta* **2009**, *649*, 141–157.

(15) Chainani, E. T.; Choi, W. – H.; Ngo, K. T.; Scheeline, A. *Anal. Chem.* **2014**, *86*, 2229–2237.

(16) Pierre, Z. N.; Field, C. R.; Scheeline, A. *Anal. Chem.* **2009**, *81*, 8496–8502.

(17) Westphall, M. S.; Jorabchi, K.; Smith, L. M. *Anal. Chem.* **2008**, *80*, 5847–5853.

(18) Hyk, W.; Nowicka, A.; Misterkiewicz, B.; Stojek, Z. *J. Electroanal. Chem.* **2005**, *575*, 321–328.

DOI: 10.1021/acs.analchem.7b01533
Anal. Chem. 2017, 89, 8057–8063

(19) Cooper, J. B.; Bond, A. M.; Oldham, K. B. *J. Electroanal. Chem.* **1992**, *331*, 877−895.
(20) Aoki, K.; Tokida, A. *Electrochim. Acta* **2000**, *45*, 3483−3488.
(21) Ciszkowska, M.; Stojek, Z. *Anal. Chem.* **2000**, *72*, 754A−760A.
(22) Afkhami, A.; Ghaedi, H.; Madrakian, T.; Nematollahi, D.; Mokhtari, B. *Talanta* **2014**, *121*, 1−8.
(23) Bueno, P. R.; Goncalves, L. M.; dos Santos, F. C.; dos Santos, M. L.; Barros, A. A.; Faria, R. C. *Anal. Lett.* **2013**, *46*, 258−265.
(24) Torres, R.; Jimenez, Y.; Arnau, A.; Gabrielli, C.; Joiret, S.; Perrot, H.; To, T. K. L.; Wang, X. *Electrochim. Acta* **2010**, *55*, 6308−6312.
(25) Thiemig, D.; Bund, A.; Talbot, J. B. *Electrochim. Acta* **2009**, *54*, 2491−2498.
(26) Campos, E. A.; Dutra, R. C. L.; Rezende, L. C.; Diniz, M. F.; Nawa, W. M. D.; Iha, K. *J. Aerosp. Technol. Manag.* **2010**, *2*, 323−330.
(27) Gougaud, C.; Rai, D.; Delbos, S.; Chassaing, E.; Lincot, D. *J. Electrochem. Soc.* **2013**, *160*, D485−D494.
(28) Castillo, C. E.; Armstrong, J.; Laurila, E.; Oresmaa, L.; Haukka, M.; Chauvin, J.; Chardon-Noblat, S.; Deronzier, A. *ChemCatChem* **2016**, *8*, 2667−2677.
(29) Khan, J.; Tripathi, B. P.; Saxena, A.; Shahi, V. K. *Electrochim. Acta* **2007**, *52*, 6719−6727.
(30) Armstrong, R. D.; Todd, M.; Atkinson, J. W.; Scott, K. *J. Appl. Electrochem.* **1997**, *27*, 965−969.
(31) Liu, Y.-L.; Ye, G. − A.; Yuan, L. − Y.; Liu, K.; Feng, Y. − X.; Li, Z. − J.; Chai, Z. − F.; Shi, W. Q. *Electrochim. Acta* **2015**, *158*, 277−286.
(32) Griess, J. C.; Rogers, L. B. *J. Electrochem. Soc.* **1949**, *95*, 129−144.
(33) Habibi, D.; Pakravan, N.; Nematollahi, D. *Electrochem. Commun.* **2014**, *49*, 65−69.
(34) Asghari, A.; Ameri, M.; Radmannia, S.; Rajabi, M.; Bakherad, M.; Nematollahi, D. *J. Electroanal. Chem.* **2014**, *733*, 47−52.
(35) Makarem, S.; Fakhari, A. R.; Mohammadi, A. A. *Anal. Bioanal. Chem. Res.* **2015**, *2*, 85−89.
(36) Khan, Z. U. H.; Chen, Y.; Khan, S.; Kong, D.; Liang, M. H.; Wan, P.; Jin, X. *Int. J. Electrochem. Sci.* **2014**, *9*, 4665−4674.
(37) Challier, L.; Miranda-Castro, R.; Marchal, D.; Noel, V.; Mavre, F.; Limoges, B. J. *J. Am. Chem. Soc.* **2013**, *135*, 14215−14228.
(38) Kundys, M.; Adamiak, W.; Jonsson-Niedziolka, M. *Electrochem. Commun.* **2016**, *72*, 46−49.
(39) Cserey, A.; Gratzl, M. *Anal. Chem.* **1997**, *69*, 3687−3692.
(40) Male, K. B.; Luong, J. H. T. *Electrophoresis* **2003**, *24*, 1016−1024.
(41) Dam, V. A. T.; Olthuis, W.; van den Berg, A. *Analyst* **2007**, *132*, 365−370.
(42) Islam, M. M.; Ueno, K.; Juodkazis, S.; Yokota, Y.; Misawa, H. *Anal. Sci.* **2010**, *26*, 13−18.
(43) Islam, M. M.; Ueno, K.; Misawa, H. *Anal. Sci.* **2010**, *26*, 19−24.
(44) Ino, K.; Kanno, Y.; Nishijo, T.; Komaki, H.; Yamada, Y.; Yoshida, S.; Takahashi, Y.; Shiku, H.; Matsue, T. *Anal. Chem.* **2014**, *86*, 4016−4023.
(45) Han, D.; Kim, Y. − R.; Kang, C. M.; Chung, T. D. *Anal. Chem.* **2014**, *86*, 5991−5998.
(46) Zevenbergen, M. A. G.; Krapf, D.; Zuiddam, M. R.; Lemay, S. G. *Nano Lett.* **2007**, *7*, 384−388.
(47) Zevenbergen, M. A. G.; Singh, P. S.; Goluch, E. D.; Wolfrum, B. L.; Lemay, S. G. *Anal. Chem.* **2009**, *81*, 8203−8212.
(48) Zevenbergen, M. A. G.; Singh, P. S.; Goluch, E. D.; Wolfrum, B. L.; Lemay, S. G. *Nano Lett.* **2011**, *11*, 2881−2886.
(49) Wolfrum, B.; Zevenbergen, M.; Lemay, S. *Anal. Chem.* **2008**, *80*, 972−977.
(50) Rassaei, L.; Mathwig, K.; Kang, S.; Heering, H. A.; Lemay, S. G. *ACS Nano* **2014**, *8*, 8278−8284.
(51) Dumitrescu, I.; Yancey, D. F.; Crooks, R. M. *Lab Chip* **2012**, *12*, 986−993.
(52) Anderson, M. J.; Crooks, R. M. *Anal. Chem.* **2014**, *86*, 9962−9969.
(53) Amatore, C.; Da Mota, N.; Lemmer, C.; Pebay, C.; Sella, C.; Thouin, L. *Anal. Chem.* **2008**, *80*, 9483−9490.
(54) Amatore, C.; Belotti, M.; Chen, Y.; Roy, E.; Sella, C.; Thouin, L. *J. Electroanal. Chem.* **2004**, *573*, 333−343.
(55) Dumitrescu, I.; Crooks, R. M. *Proc. Natl. Acad. Sci. U. S. A.* **2012**, *109*, 11493−11497.
(56) Liang, Y.; Li, Y.; Wang, H.; Zhou, J.; Wang, J.; Regier, T.; Dai, H. *Nat. Mater.* **2011**, *10*, 780−786.
(57) Suntivich, J.; May, K. J.; Gasteiger, H. A.; Goodenough, J. B.; Shao-Horn, Y. *Science* **2011**, *334*, 1383−1385.
(58) Gong, K.; Du, F.; Xia, Z.; Durstock, M.; Dai, L. *Science* **2009**, *323*, 760−764.
(59) Chung, H. T.; Won, J. H.; Zelenay, P. *Nat. Commun.* **2013**, *4*, 1922.
(60) Bonakdarpour, A.; Lefevre, M.; Yang, R.; Jaouen, F.; Dahn, T.; Dodelet, J. − P.; Dahn, J. R. *Electrochem. Solid-State Lett.* **2008**, *11*, B105−B108.
(61) Rozniecka, E.; Jonsson-Niedziolka, M.; Celebanska, A.; Niedziolka-Jonsson, J.; Opallo, M. *Analyst* **2014**, *139*, 2896−2903.
(62) Kneten, K. R.; McCreery, R. L. *Anal. Chem.* **1992**, *64*, 2518−2524.
(63) Wang, J.; Musameh, M. *Analyst* **2004**, *129*, 1−2.
(64) Bard, A. J.; Faulker, L. R. *Electrochemical Methods*, 2nd ed.; Wiley: New York, 2001.
(65) Chen, W.; Chen, S. *Angew. Chem., Int. Ed.* **2009**, *48*, 4386−4389.
(66) Liu, R.; Wu, D.; Feng, X.; Mullen, K. *Angew. Chem.* **2010**, *122*, 2619−2623.
(67) Ni, J.-A.; Ju, H.-X.; Chen, H.-Y.; Leech, D. *Anal. Chim. Acta* **1999**, *378*, 151−157.
(68) Kneten, K. R.; McCreery, R. L. *Anal. Chem.* **1992**, *64*, 2518−2524.
(69) The theoretical collection efficiency is 42% according to: Bard, A. J.; Faulker, L. R. *Electrochemical Methods*, 2nd ed.; Wiley: New York, 2001.

DOI: 10.1021/acs.analchem.7b01533
Anal. Chem. 2017, 89, 8057−8063